

Transformation behavior of prism shaped shape memory alloy single crystals

V. Novák^{a,*}, P. Šittner^a, S. Ignacová^{a,b}, T. Černoš^{a,b}

^a Institute of Physics AS CR, Na Slovance 2, 18221 Prague 8, Czech Republic

^b Faculty of Nuclear Sciences and Physical Engineering, CTU, Břehová 7, 11519 Prague, Czech Republic

Received 26 April 2005; received in revised form 25 January 2006; accepted 28 February 2006

Abstract

A methodology of successive compression loads to different faces of a prism shaped SMA single crystal is proposed as an efficient approach to investigate twinning deformation processes in martensites. It is applied to study twinning processes in 2H martensite phase in Cu–Al–Ni single crystals. The method involves an experimental evaluation of compression stress–strain curves, a measurement of complete shape changes due to transformation and twinning processes, and a three surface trace analysis for characterization of planar interfaces. The experiments are supported by theoretical calculations of shape change, analysis of the possible twinning modes and orientation dependence of twinning stresses. It was found that the large difference between the resolved shear stresses for type II (7 MPa) and compound twinning (0.7 MPa) and their orientation dependencies control the stress–strain responses of the 2H martensite in uniaxial compression. Type I twinning was not observed in compression. It is reported that the reversion of the martensite variant single crystal to the austenite upon heating proceeds very fast along a rather complex reverse transformation path at a temperature $T = \sim A_s + 40$ K.

© 2006 Elsevier B.V. All rights reserved.

Keywords: Cu-based SMAs; Single crystal; Martensite; Compression; Twinning deformation

1. Introduction

Shape memory alloys (SMAs) exhibit a variety of deformation processes derived from martensitic phase transformation. While the phase transformation processes in commonly used SMAs have been thoroughly investigated [1–3], less information is available on elastic properties of martensites, twinning processes in martensites and transitions between different types of martensites [1,2]. Most of the research papers in SMA modelling field have focused the phase transformation processes but the twinning processes in martensites are equally important. The lack of knowledge concerning the elastic properties and deformation processes in martensites seems to become a problem for modelling of the shape memory phenomena involving martensitic transformation as well as martensite deformation. More experimental and theoretical research on elastic properties of martensitic phases and twinning processes in martensite is clearly needed.

The aim of this work is to present results of a systematic experimental investigation of transformation and twinning processes in Cu–Al–Ni alloy using a novel approach consisting in sequential loading of prism shaped single crystal samples in compression. Extensive studies of phase transformation processes in Cu–Al–Ni single crystals were carried out ~25 years ago by various groups in Japan, Europe and Argentina (for recent review see [3]). Most of the experiments were carried out in tension and provided essential textbook information on physics, crystallography, thermodynamics and mechanics of martensitic transformations in Cu–Al–Ni. Recently, experimental studies of deformation processes in SMA single crystals have appeared in the literature again (e.g. [4,8]), motivated by a need for material data to be used in micromechanics modelling of SMAs. As pointed out above, only few results concerning twinning processes in 2H martensite in Cu–Al–Ni single crystals exist in the literature [5–8]. Structure [2], elastic constants [9–11] and twinning processes [6] in 2H martensite phase are known. Change of elastic properties (elastic constants) with stress induced cubic–2H orthorhombic transformation in Cu–Al–Ni single crystal was reported recently [10]. Information is missing on twinning stresses, anisotropy and effect of sense of load on the twinning processes in 2H martensite phase. The reasons that motivated us

* Corresponding author. Tel.: +42 266 052604; fax: +42 286 890 527.
E-mail address: novakv@fzu.cz (V. Novák).

to make compression experiments on prism shaped single crystal samples include: (i) compression test data on twinning are scarce; (ii) grip constraint effects on the large shape changes due to twinning are relatively limited in compression tests; (iii) one sample can be beneficially deformed successively along three load axes (three prism faces); (iv) shape change of the crystal due to twinning can be precisely evaluated. A disadvantage is that the prism shape is not optimal for compression test. The stress state in the sample is not exactly uniaxial and the orientation of the load axis varies during the compression tests.

2. Experiment

A single crystal of Cu–14.3Al–4.2Ni (wt.%) alloy was grown by use of the Bridgman method. The transformation temperatures were determined by differential scanning calorimetry (DSC) as M_s (2H) \sim 248 K and A_s \sim 285 K (Fig. 1(a)). Due to the thermal hysteresis and a shift of A_s due to deformation (see below), such crystal may exist at room temperature either in the bcc austenite or in the 2H martensite phases. Specimens were spark cut in the austenitic phase in a cuboid shape with various

crystallographic orientations of parallel faces and dimensions (see Table 1 for details of the sample used in this work). The cuboid shape of the austenite sample changed into one of the six possible martensite prism shapes (opposite sample faces are still parallel but have different normal distances and contain general edge angles, Fig. 1(b)), depending on which martensite variant has formed in the compression tests (see Section 3.3 for details). Specimen faces were carefully polished in the austenitic state at $T=330$ K. The crystal lattice orientations were determined by the back-reflection Laue method.

Compression tests were performed in an INSTRON 1362 electromechanical testing machine at room temperature using strain rates ranging from 4×10^{-5} to $4 \times 10^{-3} \text{ s}^{-1}$. Since the shape change of the SMA single crystal during compression tests is large, it is crucial to try to avoid sample-grip constraint effects as much as possible. Therefore, contact faces of the compression grips were made exactly parallel, polished and slightly lubricated. Moving traces of interfaces on polished surface were observed *in situ* by an optical microscope mounted on the frame of testing machine. After the test (when needed also during test interrupts) a detailed evaluation of the shape of sample and ori-

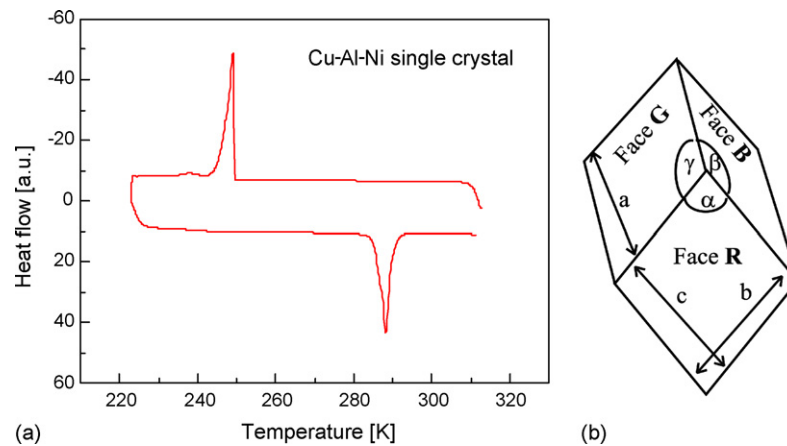


Fig. 1. (a) DSC scan of the Cu–Al–Ni sample, (b) geometrical parameters a , b , c , α , β , γ , (distances between parallel faces and edge angles) used to characterize the prism shape of the sample in austenite and martensite states. Three faces of the prism are denoted as red (R), green (G), blue (B) for easy manipulation with the sample during the compression sequences. (For interpretation of the references to color in this figure legend, the reader is referred to the web version of the article.)

Table 1
Comparison of experimental and calculated shapes (see Fig. 1(b) for definition of geometrical parameters a , b , c , α , β , γ) and face normals (direction cosines in bases of austenite and martensite lattices) of austenite and martensite single variant crystals (V2, V1, V5)

| | Dimensions (mm) | | | Edge angles ($^\circ$) | | | Face normals | | | | | | | | |
|-----------------------|-----------------|-------|-------|--------------------------|---------|----------|--------------|---------|---------|---------|---------|---------|---------|---------|---------|
| | a | b | c | α | β | γ | R | B | G | | | | | | |
| Austenite | | | | | | | | | | | | | | | |
| Experimental | 5.572 | 5.945 | 6.595 | 89.0 | 88.6 | 90.4 | -0.3003 | -0.7310 | -0.6127 | -0.9550 | 0.1986 | 0.2205 | 0.0627 | -0.6370 | 0.7683 |
| Martensite variant V2 | | | | | | | | | | | | | | | |
| Experimental | 5.655 | 5.526 | 6.964 | 88.5 | 89.2 | 93.6 | | | | | | | | | |
| Calculated | 5.641 | 5.504 | 6.996 | 88.4 | 88.1 | 93.9 | -0.0797 | -0.3313 | -0.9402 | -0.0135 | -0.9633 | 0.2682 | -0.9927 | 0.0724 | 0.0962 |
| Martensite variant V1 | | | | | | | | | | | | | | | |
| Experimental | 5.820 | 5.543 | 6.755 | 88.7 | 90.1 | 94.5 | | | | | | | | | |
| Calculated | 5.827 | 5.518 | 6.746 | 88.4 | 88.9 | 95.1 | 0.9357 | -0.3422 | -0.0855 | -0.2590 | -0.9658 | -0.0141 | -0.0894 | 0.0699 | -0.9935 |
| Martensite variant V5 | | | | | | | | | | | | | | | |
| Experimental | 5.594 | 6.108 | 6.333 | 90.7 | 83.1 | 87.2 | | | | | | | | | |
| Calculated | 5.555 | 6.109 | 6.343 | 90.0 | 81.6 | 87.0 | 0.6847 | -0.6657 | 0.2968 | -0.8004 | 0.2504 | -0.5447 | 0.4493 | 0.8072 | -0.3828 |

entation of the surface traces was made. Cooling–heating experiments inside the optical microscope were made using a Peltier table. In some cases, in order to slow down the transformation kinetics for *in situ* optical observations, the cooling–heating was made in a temperature gradient achieved by active cooling of upper face of the sample while heating the lower face at the same time.

The prism shape of the sample (different for each particular martensite single crystal variant existing in it) was calculated [12] from original shape of the austenitic sample, lattice parameters of austenite (bcc: $a_0 = 0.5835$ nm) and martensite (orthorhombic 2H: $a = 0.4389$ nm, $b = 0.5342$ nm, $c = 0.4224$ nm), lattice correspondence and shape strain of the martensitic transformation [2]. Crystallographic orientations of habit planes and twinning planes were determined by three surface trace analysis on partially deformed samples.

3. Results and discussion

3.1. Thermally induced austenite–martensite transition

Martensitic transformation taking place in the crystal thermally cycled at zero stress proceeds via formation of multiple variants of 2H martensite. Since mutual accommodation of shape strains of individual variants was never perfect, the prism sample slightly changed its shape with the transformation, each cycle, however, differently. Moving traces of habit plane variants

of twinned 2H martensite phase ranging from tens up to hundreds of micrometers in size were observed *in situ* on polished sample surfaces. If the sample was carefully cooled in a thermal gradient, however, it was possible to achieve martensitic transformation proceeding via slow motion of a single habit plane interface between austenite and twinned 2H martensite phase in a repetitive manner. Thermally induced transformations are, however, not focused in this work.

3.2. Stress-induced austenite–martensite transition

Stress-induced martensitic transformation was observed upon loading the prism in the austenite phase at room temperature. The recorded stress–strain curves [8,10] depended significantly on the specimen orientation (crystallographic indexes of the normal to the prism face in contact with grips). In case of load axis orientation: (i) near $[1\ 0\ 0]$, a complete transition to the 2H martensite phase that remained stable after unloading (Figs. 2(a) and 3(a)) was observed; (ii) near $[1\ 1\ 0]$, the sample response was usually pseudoelastic (into a mixture of stress induced 2H and 18R martensites) with the hysteresis of about 200 MPa [8]; (iii) near $[1\ 1\ 1]$, the transformation strain was relatively low and transformation stress high, so that only partial transformation upon loading up to 400 MPa could be achieved, in some cases, there was only elastic deformation. Frequently, a single detwinned variant formed at the end of compression test (Figs. 2(a) and 3(a)). However, if the load axis

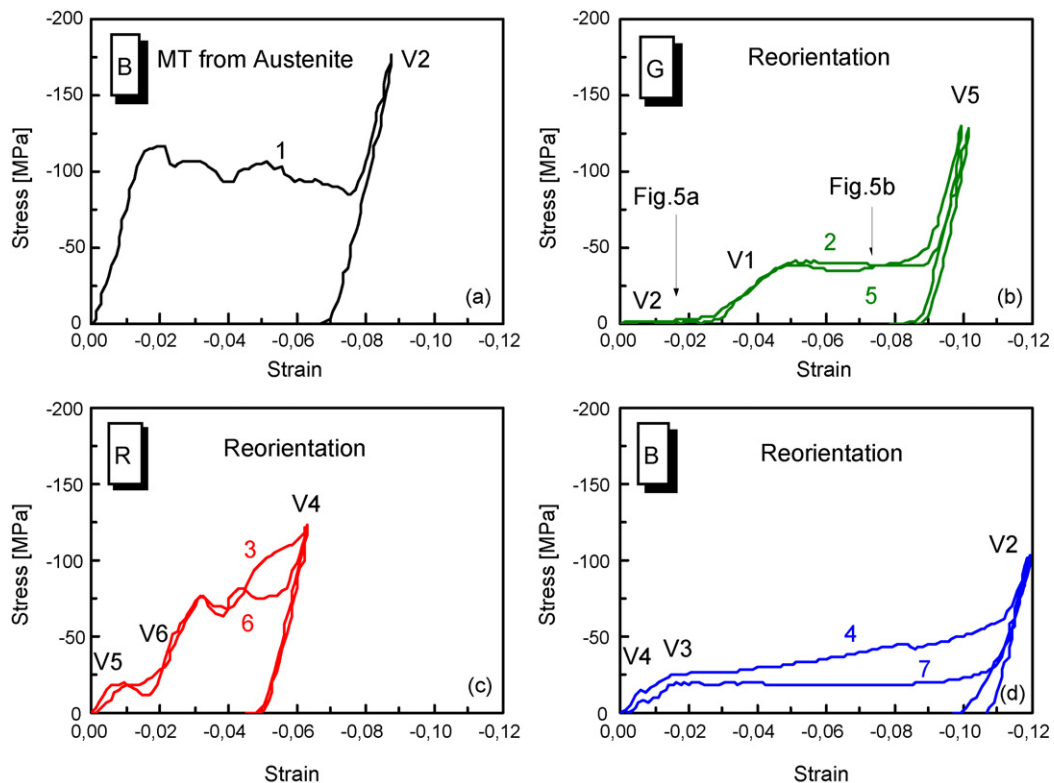


Fig. 2. Stress–strain curves of Cu–Al–Ni single crystal at room temperature recorded during a sequence BGRBGRB of compression loads (curves numbered sequentially 1–7) starting by compression on the face B of originally austenite prism (a), turning the sample $\sim 90^\circ$ and compressing on the face G (curve 2 in (b)), etc. V1–V6 denote which variant exists in the sample at corresponding strain. (For interpretation of the references to color in this figure legend, the reader is referred to the web version of the article.)

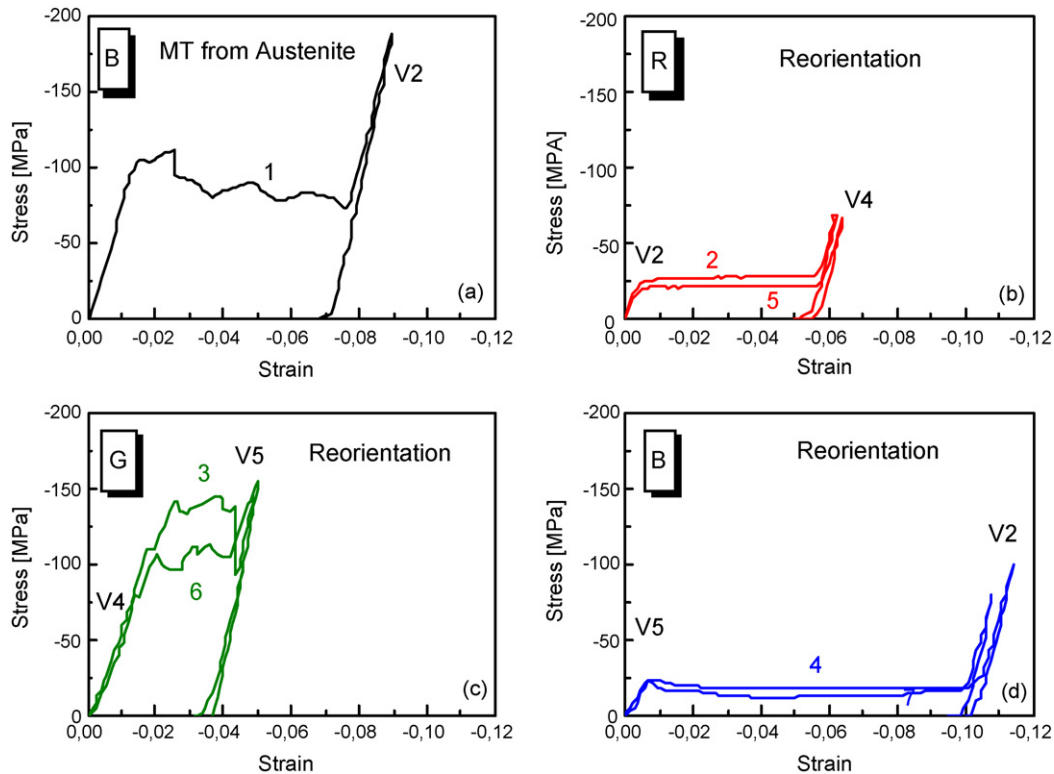


Fig. 3. Stress–strain curves of Cu–Al–Ni single crystal at room temperature recorded during a sequence BRGBRGB of compression loads (curves numbered sequentially 1–7) starting by compression on the face B of originally austenite prism (a), turning the sample $\sim 90^\circ$ and compressing on the face R (curve 2 in (b)), etc. V1–V6 denote which variant exist in the sample at corresponding strain. (For interpretation of the references to color in this figure legend, the reader is referred to the web version of the article.)

orientation was located close to the $001-011-111$ symmetry zones, two or more variants sometimes formed and it was not possible to obtain martensite variant single crystals even by loading up to 500 MPa. This is due to the orientation and sense of load dependences of cubic-orthorhombic and cubic-monoclinic transformations in compression [8]. More information on stress-induced martensitic transformations in Cu–Al–Ni single crystals in tension/compression can be found in our earlier papers [8,13].

3.3. Martensite reorientation

The methodology of compression experiments on shape memory prisms brings a real benefit namely for the research of martensite reorientation (twinning) processes. Particularly, when the martensite prism obtained as a result of stress induced transformation at room temperature (Figs. 2(a) and 3(a)) is turned to align a different sample face normal with the compression load axis, the prism can be deformed at relatively low stress (Figs. 2(b) and 3(b)) again. This time, although the temperature has not changed, the sample deforms via twinning deformation in the 2H martensite phase (martensite reorientation, Figs. 2(b)–(d) and 3(b)–(d)). For easy manipulation, three different faces of the prism sample are denoted R, G and B according to the red, green and blue markings on the sample faces (Fig. 1(b)). Following a closed sequence of compression loads on different faces more than twice, quite stable responses (good reproducibility of reorientation strains and stresses in plateaus

of the σ – ε curves) were observed. The twinning stresses usually decrease in the second round of compressions and remain practically constant in the third and further rounds. The stress–strain responses for sequences BGRBGRB (Fig. 2) and BRGBRGB (Fig. 3) in the first two rounds are presented and discussed below. However, there are more possibilities regarding the selection of the compression sequences (e.g. RBRBGR, RBGRBGR, RBRBR, RBGBG, etc.).

The compression sequence methodology partially solves an essential problem of the history dependence encountered in the martensite deformation studies. As very well known to SMA experimentalists, any stress–strain curve of a SMA sample in the martensite state (single crystal or polycrystal) depends very much on the previous deformation history (on the martensite variant microstructure existing in the sample prior to the test). In order to deduce meaningful information from an experimentally measured martensite reorientation stress–strain curve, the sample state prior to the test must be well defined. Let us point out that simple stress free cooling does not necessarily lead to the well defined martensite variant microstructure. By performing compression sequences in closed cycles repetitively, we achieve a situation, where the martensite sample passes through multiple well defined states (martensite variant single crystals) existing always when the crystal is deformed beyond each of the stress plateaus in Figs. 2 and 3. Martensite twinning processes (Fig. 5) take place at the strains within the stress plateaus (Fig. 2(b)). By running various sequences on a single Cu–Al–Ni sample,

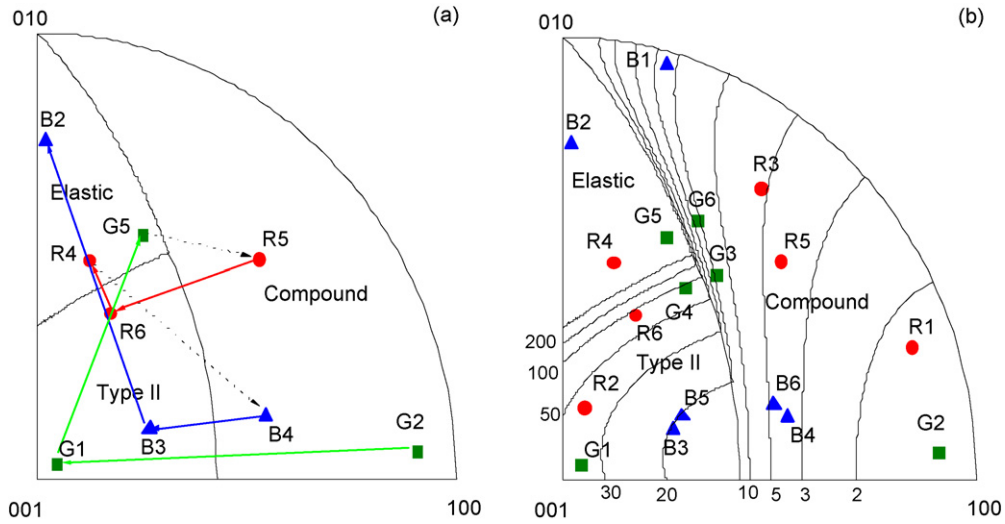


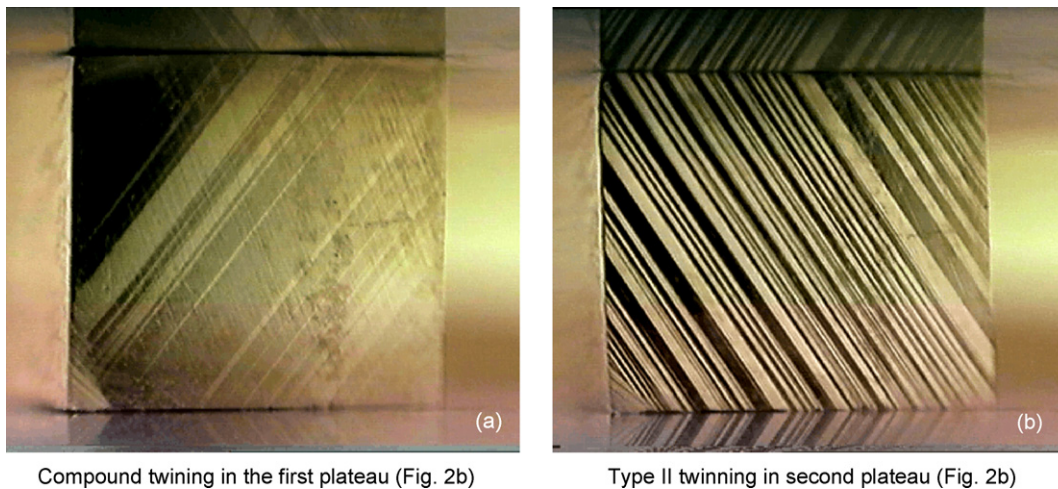
Fig. 4. Orientations of the compression load axis in 2H martensite lattice coordinates during compression loads on different faces (● red, ▲ blue, ■ green) of prism shaped Cu–Al–Ni sample. (a) Variation of the load axis during the sequence BGRBGRB in Fig. 2 starting from G2 (compression on the green face in martensite variant V2). Solid lines denote the discontinuous change of the load axis orientation due to twinning, dashed lines due to turning the sample on another face before the next compression load. Calculated boundaries separating regions where individual deformation modes appear are denoted. All load axis orientations achieved with this sample (18) and calculated equistress lines for compound, type II twinning modes are shown in (b). (For interpretation of the references to color in this figure legend, the reader is referred to the web version of the article.)

one can measure multiple compression stress–strain curves with well defined starting microstructure (martensite variant single crystals denoted V1–V6) for various load axis orientations with respect to the orthorhombic lattice (Fig. 4). Orientation dependence of twinning in 2H martensite can thus be beneficially investigated using only one specimen.

Let us further on consider only the stable stress–strain responses and look in more detail on the twinning deformation processes in the 2H orthorhombic martensite. The twinning processes are evidenced *in situ* by optical observation of parallel narrow bands of another 2H variant on the specimen surface (Fig. 5). First bands appearing beyond the knee points on the stress–strain curves are only few micrometers wide and hundreds of micrometers apart. As the strain increases during the

stress plateaus, the width of the existing bands increases and new ones appear so long the sample becomes a single crystal of the new 2H variant. If there are two sequential plateaus on the stress–strain curve (Fig. 2(b)), two sequential twinning processes (Fig. 5(a) and (b)) are observed *in situ* as moving bands of completely different inclination.

The stress–strain curves in Figs. 2 and 3 were recorded during two different sequences of compression loads on the specimen, the dimensions of which are given in Table 1. The stress strain–curves measured are numbered sequentially. The loading direction (face upon which the compression load is applied) is denoted in the upper left corner in Figs. 2 and 3. The sequences in Figs. 2 and 3 starts with compression on face B in austenite state, but the first sequence in Fig. 2 continues as GRBGRB



Compound twinning in the first plateau (Fig. 2b)

Type II twinning in second plateau (Fig. 2b)

Fig. 5. Two snapshots from a video-record taken from the red face of the prism sample undergoing two-stage deformation in compression test (Fig. 2(b)). Compression axis (green) is in vertical direction. Mirror image of the twin bands is visible on polished grip surfaces. (For interpretation of the references to color in this figure legend, the reader is referred to the web version of the article.)

while the second in Fig. 3 as RGBRGB. At the end of each plateau, the sample exists in one of the six possible lattice correspondent variants of the orthorhombic structure V1–V6 and has a characteristic shape (described by six geometric parameters $a, b, c, \alpha, \beta, \gamma$) and crystallographic orientation (direction cosines of face normals) given in Table 1 (see [10] for details). The geometrical parameters were systematically measured after unloading beyond the end of the plateaus on σ – ε curves. For demonstration, the results for the first martensite loading of the first sequence (compression on the green face in Fig. 2(b), variants V2, V1, V5) are compared with the results of theoretical calculations in Table 1. The starting variant V2 reorients by compound twinning in the first plateau (Fig. 5(a)) into variant V1 and subsequently by type II twinning in the second plateau (Fig. 5(b)) into variant V5. Main benefit of the newly introduced shape change measurements is that the martensite variants existing in the sample can be unambiguously determined. This was sometimes controversial based solely on the X-ray Laue data in earlier tensile tests [19].

The orientation of the load axis (crystallographic orientation of the normals to faces G, R, B) changes as the specimen undergoes twinning deformations in each stress–strain curve ending always in the region of orientation space denoted as *Elastic* (Fig. 4(a)). The sample orientations were experimentally measured by X-ray Laue method and compared with the calculated values (see also [10]). Fig. 4(a) shows how the load axis orientation varies during the sequence of compression loads GRBGRB—sequence of σ – ε curves 2–7 in Fig. 2 starting by compression on the green face in martensite variant V2 can be followed along the path in orientation space denoted by arrows (see Fig. 4 caption for details). By applying different sequences, deformations along multiple different load axis orientations (up to 18) can be achieved using the same single crystal. These are summarized in Fig. 4(b). The figure also shows the equistress lines calculated from resolved shear stresses (0.7 MPa for compound and 7 MPa for type II twinning modes), lattice parameters and load axis orientations [12]. The calculations are analogical to the Schmid factor calculations for twinning reported in [6,16]. Taking into account the problems with grip constraints, the theoretical twinning stress values reasonably agree with the experimental plateau stress levels of the σ – ε curves in Figs. 2 and 3. Calculated boundaries in orientation space between regions in which the oriented 2H martensite crystal undergoes compound, type II twinning modes or remains elastic are shown in Fig. 4(b) as well. The activated twinning modes [14,15] were experimentally evaluated from the twinning plane orientations determined by the trace analysis on unloaded samples. It can be concluded that: (i) compound twinning mode ($(101)_{2H}$ twinning plane) proceeds at low stress level (>1 MPa); (ii) type II twinning (no rational twinning plane) takes place at higher stress level (>15 MPa); (iii) type I twinning was not observed at all.

In several hundreds of compression tests we have found only compound and type II twinning modes, but no type I twinning. The resolved shear stresses for twinning in 2H martensite were earlier reported by Otani et al. [6] and Ichinose et al. [16], who observed an activity of the type I twinning in ten-

sion with resolved shear stress ~ 20 MPa [16]. As regards its absence in compression, the theoretical calculations [12] show that the resolved shear stress for type I twinning would have to be similar to that for the type II twinning (<8 MPa) in order to appear in compression. Probably this is not the case.

3.4. Reverse transformation from martensite single variant crystal upon heating

Reverse martensitic transformation taking place upon stress free heating of any martensite variant single crystal deserves a special attention. As follows from the DSC (Fig. 1(a)), A_s temperature for the reverse transformation from martensite to austenite shall be approximately 285 K. However, when the detwinned 2H martensite variant crystal was heated, the A_s temperature appeared to be shifted up to $T = \sim 325$ K [17] and the transformation proceeded so fast that the prisms tended to jump out of the Peltier heating stage. Of course, no microstructure evolution during heating could be video-recorded. In the following thermal cycle, the prisms transformed back to the austenite at $T = 285$ K in accordance with the DSC.

Since we were interested in the microstructure evolution upon the first heating, we utilized the temperature gradient method to slow down the transformation rate (upper face of the sample was actively cooled while bottom one was heated). In that case, the surface pattern evolution upon heating could be monitored. As illustrated in Fig. 6, the reverse transformation of the martensite variant single crystal clearly proceeds via two successive processes. At first, the twinned 2H martensite forms from the detwinned crystal via motion of the first macroscopic interface HP1. Next, the internally twinned martensite transforms to the austenite single crystal via motion of the second macroscopic interface HP2. The reverse transformation thus proceeded via an apparent motion of a twinned martensite band (Fig. 6(b)) through the crystal. This is a completely different microstructure pattern from that observed during the thermal gradient heating in stress free thermal cycles (Section 3.1) where only single macroscopic interface between the twinned martensite and austenite always moved. Let us only briefly comment on this behavior. The problem with the reverse transformation of the detwinned crystal is that no habit plane can exist between austenite and martensite single crystals. The reverse transformation hence proceeds first by formation of the twinned martensite band from which the habit plane to final austenite crystal can form. The nucleation of the twinned martensite band (in fact a kind of “martensite twinning driven by heating”) requires significant overheating of the sample above the A_s temperature. However, once the band has nucleated (making acoustic effects), both macroscopic interfaces move extremely fast (in nearly homogeneous temperature field) through the crystal.

We believe that this “complex transformation path” from the deformed martensite to the austenite is in fact one of the main reasons for various “first cycle effects”, “stabilization of martensite by deformation”, etc. reported frequently in the SMA literature [20]. Since deformation in the martensite state always leads to a partial detwinning, upward shifts of the A_s temperatures upon heating after deformation are commonly observed

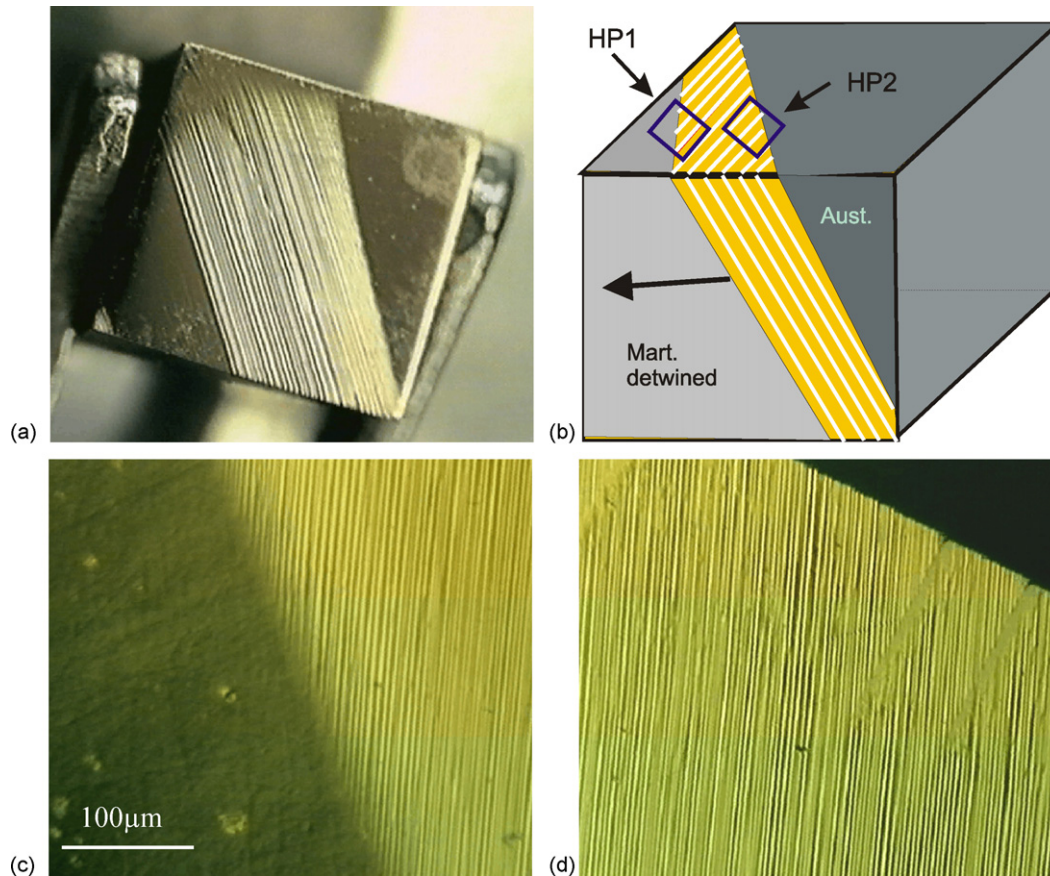


Fig. 6. Reverse transformation of the martensite variant single crystal during heating in a temperature gradient, (a) macro-view of the transforming prism sample, (b) sketch showing the two habit plane interfaces HP1 separating the original 2H martensite single variant crystal from internally twinned crystal and HP2 between the twinned martensite and austenite, (c) detailed view of the HP1, and (d) detailed view of the HP2. The twinned band moves leftwards upon heating as suggested by the arrow in (b).

in SMA experiments. An interesting point is that for the same cubic-orthorhombic transformation in various Cu-based alloys, the A_s temperature shifts are very different. While the upward shift was about ~ 40 K in the present Cu–Al–Ni crystals, it was ~ 100 K in a high-temperature Cu–Al–Ni alloy or Cu–Al–Mn alloy [17,18].

4. Conclusions

Deformation and transformation processes in Cu–Al–Ni single crystals were studied using a newly developed methodology of successive compression loads to different faces of prism shaped specimens and heating/cooling with intentional temperature gradient to slow down transformation kinetics.

The method involves experimental evaluation of compression stress–strain curves, measurement of complete shape changes due to transformation and twinning processes and three surface trace analysis for characterization of planar interfaces supported by theoretical calculations of shape change, analysis of the possible twinning modes and orientation dependence of twinning stresses. The method has been found particularly suitable for investigation of the twinning processes in the 2H orthorhombic martensite phase.

Among the three possible twinning processes in the 2H martensite structure, type I, type II and compound twinning, only the latter two were observed in compression. The resolved shear stresses for the type II (7 MPa) and compound twinning (0.7 MPa) differ significantly. The reported orientation dependence of transformation stresses and strains for both twinning modes complies with the Schmid law in the first approximation.

It is shown that the reverse transformation of the martensite single variant crystal upon heating proceeds through a very fast motion of a band of internally twinned martensite phase separated from the martensite single variant crystal on one side and austenite on the other side by two macroscopic habit plane interfaces. Reverse transformation via this rather complex reverse transformation path (in contrast to single habit plane motion observed in stress free thermal cycles) requires significant over-heating above the characteristic A_s temperature of the alloy.

Acknowledgements

Support from the Grant Agency of Academy of Sciences (project no. A1048107), Czech Science Foundation (project no. 101/06/0768) and Marie-Curie RTN Multimart (contract no. MRTN-CT-2004-505226) are greatly acknowledged.

References

- [1] K. Otsuka, H. Sakamoto, K. Shimizu, *Acta Metall.* 27 (1979) 585–601.
- [2] K. Otsuka, C.M. Wayman, K. Nakai, H. Sakamoto, K. Shimizu, *Acta Metall.* 24 (1976) 207–226.
- [3] K. Otsuka, C.M. Wayman, in: K. Otsuka, C.M. Wayman (Eds.), *Shape Memory Alloys*, Cambridge University Press, 1998.
- [4] K. Gall, H. Sehitoglu, R. Anderson, I. Karaman, Y.I. Chumlyakov, I.V. Kireeva, *Mater. Sci. Eng. A* 317 (2001) 85–92.
- [5] S. Ichinose, Y. Funatsu, K. Otsuka, *Acta Metall.* 33 (1985) 1613–1620.
- [6] N. Otani, Y. Funatsu, S. Ichinose, S. Miyazaki, K. Otsuka, *Scripta Metall.* 17 (1983) 745–750.
- [7] K. Okamoto, S. Ichinose, K. Morii, K. Otsuka, K. Shimizu, *Acta Metall.* 34 (1986) 2065–2073.
- [8] V. Novák, P. Šittner, D. Vokoun, N. Zárubová, *Mater. Sci. Eng. A* 273 (1999) 280–285.
- [9] M. Yasunaga, Y. Funatsu, S. Kojima, K. Otsuka, T. Suzuki, *J. Phys.* 43 (1982) 603–608.
- [10] P. Sedlák, H. Seiner, M. Landa, V. Novák, P. Šittner, L.I. Mañosa, *Acta Mater.* 53 (2005) 3643–3661.
- [11] M. Landa, P. Sedlák, P. Šittner, H. Seiner, V. Novák, in: *Proceedings of the ISPMA 10*, *Mater. Sci. Eng. A* (2006) in press.
- [12] T. Černoč, V. Novák, P. Šittner, submitted for publication.
- [13] P. Šittner, V. Novák, *J. Eng. Mater. Technol. ASME* 121 (1999) 48–55.
- [14] K.F. Hane, T.W. Shield, *J. Elasticity* 59 (2000) 267–318.
- [15] K.F. Hane, T.W. Shield, *Proc. Roy. Soc. Lond. A* 455 (1999) 3901–3915.
- [16] S. Ichinose, Y. Funatsu, N. Otani, T. Ichikawa, S. Miyazaki, K. Otsuka, *Proceedings of the International Symposium on Intermetallic Compounds (JIMIS-6)*, Sendai, 1991, pp. 263–267.
- [17] V. Novák, P. Šittner, J. Van Humbeeck, *J. Phys. IV France* 11 (2001) Pr8-191–Pr8-196.
- [18] N. Zárubová, V. Novák, *Mater. Sci. Eng. A* 378 (2004) 216–221.
- [19] K. Okamoto, S. Ichinose, K. Morii, K. Otsuka, K. Shimizu, *Acta Metall.* 34 (1986) 2065–2073.
- [20] Y. Liu, Z. Xie, J. Van Humbeeck, L. Delaey, *Mater. Sci. Eng. A* 273–275 (1999) 679–684.